

Improvement of a bedload transport rate measuring system in sediment bypass tunnels

T. Koshiba, C. Auel, D. Tsutsumi, S.A. Kantoush & T. Sumi

Water Resources Research Center, Disaster Prevention Research Institute, Kyoto University, Uji, Japan

ABSTRACT: For long term use of dams, it is required to develop methods of sediment management in reservoirs. As one method, Sediment Bypass Tunnels (SBT) are operated in Japan and Switzerland to prevent reservoir sedimentation. SBT reduces sedimentation in reservoirs by routing the incoming sediments around the dam. SBT, however, is prone to severe invert abrasion caused by high sediment flux. Therefore, it is necessary to establish a measurement system of sediment transport rates in the SBT. A geophone was experimentally investigated in a laboratory flume at ETH Zurich. The sediment transport rate is calculated based on the plate vibration caused by hitting of gravels. In this paper, in order to alleviate disadvantages of a geophone, two newly developed sensor systems, a plate microphone and plate vibration sensor, are suggested and the results of their calibration experiments are shown. Finally, they are compared with the existing methods.

1 INTRODUCTION

1.1 Background

Many dams in the world are prone to reservoir sedimentation and require urgent sedimentation management. One advanced technique against the problem is the sediment bypass tunnel (SBT) to reduce suspended and bed load depositions in reservoirs by routing the incoming sediments around the dam (Sumi et al. 2004, Auel & Boes 2011). SBTs are an effective strategy bypassing about 80 to 94% of the incoming sediments (Auel et al. 2016). Figure 1 shows the outlet structure of the operating Solis SBT located in the Swiss Alps. However, measuring and quantifying the sediment transport in a SBT is challenging and a topical research subject (Hagmann et al. 2015). Especially invert abrasion is a severe problem facing most SBT which is directly connected to increasing maintenance cost (Auel & Boes 2011, Baumer & Radogna 2015,

Jacobs & Hagmann 2015, Nakajima et al. 2015). The invert abrasion is caused by a combination of high flow velocities and high sediment transport rates (Auel 2014). The sediment which is routed downstream of the dam during floods is also important regarding river environmental aspects. Various techniques have been developed to monitor suspended sediment, for example by using turbidity current meter. However, there are limited techniques for field observation of bedload sediment transport to understand the mechanisms and to quantify bedload transport rates (BTR).

1.2 Existing measurement techniques for BTR

To measure BTR precisely is not only prospective to contribute to the maintenance of SBTs but also meaningful from the aspect of comprehensive river basin management. As an indirect BTR measuring system, a geophone was developed in the early 1990ies in Switzerland. The geophone is mainly used in European countries especially in mountainous areas of Switzerland, Austria, and Italy (Rickenmann et al. 2012). The geophone consists of a 50 cm by 36 cm steel plate with a geophone sensor (Geospace GS-20DX, manufactured by Geospace Technologies, Houston, Texas) mounted below, embedded in a steel frame and installed directly in the river bed. A geophone estimates BTR based on the plate vibration expressed in voltage caused by the passing sediment. A geophone system was installed the first time in an SBT at the Solis dam and started operation from 2013 (Hagmann et al. 2015). At the field observation in Erlenbach in Switzerland, a good correlation between long term BTR and the output of geophone was confirmed (Rickenmann et al. 2012). Furthermore, the geophone is



Figure 1. Outlet of the Solis SBT (courtesy of C Auel).

robust against the impact of sediment and therefore feasible to be installed on the invert of a SBT. It is also revealed that, however, the geophone cannot detect fine sediments with a diameter smaller than 2 to 4 cm (Rickenmann et al. 2012). In order to clarify the effects of abrasion on the SBT invert, the impinging gravel grain size is important. This is because the amount of abrasion on the invert not only depends on the sediment flux but also the grain size.

After the development of geophones in Switzerland, another similar indirect BTR measuring system was developed in Japan, the hydrophone (Mizuyama et al. 2010). Japan also has gravel bed rivers in the mountains similar to Switzerland. The hydrophone consists of a rounded metal pipe installed directly in the river bed. When gravels and sand pass over the pipe, the number of hitting particles is counted by the hydrophone based on sound pressure. The pipe hydrophone system is already installed in some rivers in Japan and many experiments are conducted at the Hodaka Sedimentation Observatory, DPRI, Kyoto University (Tsutsumi et al. 2010). The studies at the observatory revealed that the hydrophone can detect fine sediment with a diameter larger than 4 mm. However, the hydrophone often underestimates bedload when the pulses are successive and overlap because the hydrophone does not have a large width in flow direction. Also the hydrophone easily deforms when hit by large stones negatively effecting the sound collection.

According to the discussions above, each measuring technique has the similar sediment rate measuring principle. However, both systems have different features caused by the difference of sensors and design (Tab. 1). To improve the weak points of these two techniques with leaving their advantages, a plate microphone and a new plate vibration sensor were tested. In this study, a new method to measure BTR with steel plate microphone is proposed and experimentally investigated for various hydraulic and sediment conditions.

1.3 New devices to measure BTR

A plate-microphone was developed in Japan as a method to measure the BTR to overcome disadvantages of the pipe-hydrophone as shown in Table 1. The plate-microphone system consists of a steel plate like the geophone and measures bedload transport rates based on sound pressure like the hydrophone. With these characteristics, the plate microphone is expected to record hitting sounds of fine sediment and also to be robust against hitting by coarse sediment. Additionally, below the plate also a plate vibration sensor is mounted which uses a different type of vibration sensor compared to the geophone (GA-313A as a sensor and GA-223 as a converter, manufactured by KEYENCE, Japan). Figure 2 shows the plate microphone and the plate vibration sensor installed in an experimental flume at the Laboratory of Hydraulics (VAW) at ETH Zurich. The most significant difference of the geophone and plate vibration sensor is

Table 1. Difference of the geophone and the hydrophone.



	Geophone	Hydrophone
Photo		
Merit	<ul style="list-style-type: none"> • Robust against large stones • Thicker plate can deal with larger stones up to decimetres 	<ul style="list-style-type: none"> • Inexpensive system setup • the minimum detectable grain size is 10mm to 40mm
Demerit	<ul style="list-style-type: none"> • Initial installation cost is high • Minimum detectable grain size is 10mm to 40mm 	<ul style="list-style-type: none"> • Deforms easily when large stones hit • Overestimate bedload rate during high sound or large amount of sediment



Figure 2. Plate microphone and plate vibration sensor in the test flume.

the disparity of their resonance frequency. The natural frequency of the geophone sensor is 10 Hz and the frequency is classified as ultra-low frequency. It is because the geophone sensor is designed to be used for the observation of seismic data. On the other hand, the frequency response of Japanese plate vibration sensor is 100 Hz~80 kHz and the range is much higher than the geophone ones. Due to this difference, it is expected that the plate vibration sensor is more suitable than the geophone because the impact on the rigid steel plate possesses higher frequency than ground motion.

In order to confirm this hypothesis, laboratory experiments were conducted in 2014 at ETH Zurich, the results are discussed in this paper.

2 EXPERIMENTAL SETUP

2.1 Test flume

The experiments of this study were carried out in a flume facility at the VAW hydraulic laboratory of ETH Zurich, Switzerland. A schematic view of the experimental setup and parameters are shown in Figure 3. The experimental setup consists of an elevated water

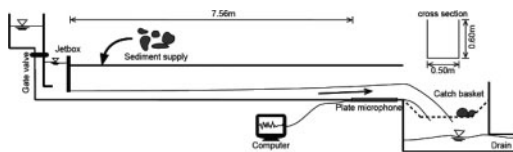


Figure 3. Schematic view of the laboratory test flume.

Table 2. Dimensions of tested sediment.

Grain size D_s [mm]	B-axis [mm]	Average Weight [g]
2	2.00–2.36	3.2 of 200 particles
5	5.00–6.00	14.3 of 100 particles
10	10.0–12.0	2.1
50	45.0–55.0	159.2
100	95.0–105.0	2937.6

supply tank that discharges the water through a jetbox (Schwalt & Hager 1992) to a rectangular glass-sided flume with inner dimensions of 0.50 m width, 0.60 m height, and 8.00 m length. The flume bed is horizontal and the water is flowing in steady-state supercritical free surface conditions. The steel plate with the microphone and plate vibration sensor are placed just before the flume outlet at 7.56 m from the inlet. The discharge is controlled by a gate valve. The flow velocity is obtained by measuring the discharge with a magnetic flow meter and the flow depth with point gauge measurements. At the flume end the water plunges into a stilling basin.

In the experiment, the plate microphone and the plate vibration sensor are installed in the same steel plate box and all experiments are measured by both measuring systems. The device consists of four parts: steel plate, a microphone, a vibration sensor and a data-logger. The geometry of the steel plate are: 49.2 cm width, 35.8 cm length, and 1.5 cm thickness. Water and sediment flows are perpendicular to the plate width. The microphone which detects the sound wave and the vibration sensor which records the vibration of the plate are installed under the plate and connected to the data-logger.

In this experiment, five types of gravels are used. Grain sizes and average weight are shown in Table 2. The sediment particle density is $\rho_s = 2700 \text{ kg/m}^3$. The tested sediment has various shapes including rounded, irregular and angular particles.

2.2 Recording systems

In accordance with the previous observations by the hydrophone (Mizuyama et al. 2008, Suzuki et al. 2010), the following three parameters were measured during each experiment: acoustic and vibration waveform, the number of pulses, as well as sound and vibration pressure. The mechanisms of these three parameters are described in the following.

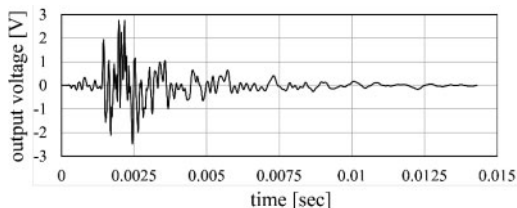


Figure 4. Example of vibration waveform.

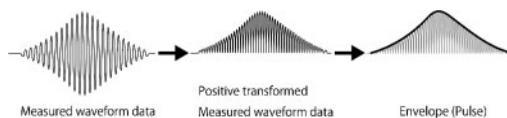


Figure 5. Process of converting raw waveform data.

2.2.1 Sound and vibration waveform

The sound waveform is raw data collected by the microphone and the vibration sensor. A value of voltage was recorded every $20 \mu\text{s}$. Figure 4 shows one example of a raw waveform output.

2.2.2 The number of pulses

The recorded parameter number of pulses I_n represents the number of gravels which hit the pate. The pulse is determined by processes shown in Figure 5. First, the raw waveform is 20-times amplified by a preamplifier and transformed into an absolute value. Then, the specific frequency of acoustic waveform data is extracted by a bandpass filter and an envelope curve of this wave is recorded as the waveform and amplified 10-times again. The envelope curve of the sound waveform is called sound pressure. Therefore, the envelope curve of the vibration waveform is called vibration pressure in this paper. The transformed data is exported to 6 different channels, in which the wave was amplified 2, 4, 16, 64, 256, and 1024 times. The amplification was made to find the best value to detect the highest number of particle impacts. Finally, the number of pulses whose amplitude is larger than the threshold value of 2V are logged by the logger. Figure 6 explains this process. However, for the vibration waveform, not the positive transformed vibration waveform but the envelope data is used to count the number of pulses because of a technical problem. Due to the difference of process between the acoustic waveform and the vibration waveform, the number of pulses of the vibration waveform is much higher than the acoustic waveform's one.

2.2.3 Acoustic energy and vibration energy

When sediment transport rate is high, the number of pulses exceeding the threshold are underestimated due to overlapping of each separated pulse. To counter this problem, the acoustic energy E_s and the vibration energy E_v are also measured. Figure 7 explains the principle. The sound pressure is the mean value of the envelope amplitude. The mean value is calculated

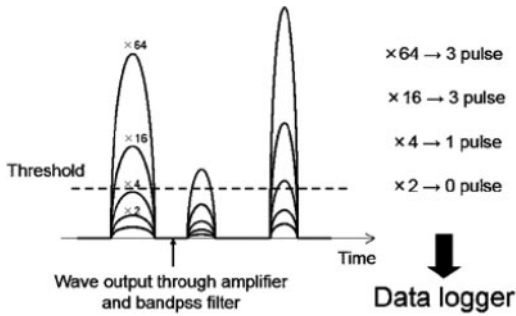


Figure 6. Process to count the number of pulses.

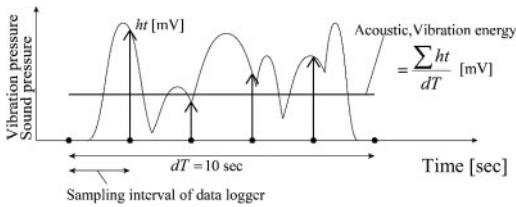


Figure 7. The principle of recording sound pressure and vibration pressure.

and recorded at 10 seconds intervals. Hence, E_s and E_v are the average value of the output voltage [mV].

2.3 Experimental conditions

The experimental conditions are presented in Table 3. The flow depth was kept constant with 0.08 m, whereas the discharge Q and velocity V were varied two times, represented as *low* and *high* flow conditions. W is the amount of sediment. Normally, the flow velocity in a SBT is higher and often reaches more than 10 m/s (Auel & Boes 2011). Gravels are released into the test flume by hand just after the jetbox. These gravels are transported along the flume, detected by the plate and caught by a basket. A constant sediment weight of 50 g for both grain sizes, $D_s = 2$ mm and 5 mm was supplied. For $D_s = 10$ mm, 50 mm, and 100 mm, a fixed number of 20 stones was added manually to the flow every five seconds. Every case was repeated 50 times, therefore in total 1000 tests were carried out.

3 RESULTS AND DISCUSSIONS

3.1 Results

3.1.1 Sound and vibration waveform

Figure 8 and Figure 9 are examples of the results of the waveforms. Figure 8 is a result of case 10 ($V = 4.5$ m/s, $D_s = 100$ mm), and Figure 9 of case 6 ($V = 4.5$ m/s, $D_s = 2$ mm). The top wave is the sound waveform and the bottom is the vibration waveform. According to Figure 8, both devices detect the impinging of gravels. The forms of them are, however, not the same. It is observed that the wave length caused by a gravel

Table 3. Experimental conditions.

Case No.	Flow		Sediment	
	Q [m ³ /s]	V [m/s]	D_s [mm]	W [g]
1	0.10	2.5 (Low)	2	50
2	0.10	2.5 (Low)	5	50
3	0.10	2.5 (Low)	10	50
4	0.10	2.5 (Low)	50	20 stones
5	0.10	2.5 (Low)	100	20 stones
6	0.18	4.5 (High)	2	50
7	0.18	4.5 (High)	5	50
8	0.18	4.5 (High)	10	50
9	0.18	4.5 (High)	50	20 stones
10	0.18	4.5 (High)	100	20 stones

hit measured by the plate microphone is much longer than the vibration sensor. To consider this difference, the plate vibration has an advantage to avoid the overlap of waves when high amount of sediment passes over it. On the other hand, it is also observed that the output voltage sometimes saturates. To confirm the problem, more experiments to clarify the maximum grain size which does not saturate is needed. Whereas, Figure 9 clearly explains the difference of the both devices when the fine sediment hit. The plate microphone can not detect $D_s = 2$ mm sediment obviously but the plate vibration sensor detects them. Actually, to expand the y-axis of the plate microphone's waveform, there is a successive wave. However, these waves appear in the water flow without sediment. Therefore these are noises of water flow and the waves of sediment concealed under the noise are hard to be confirmed.

3.1.2 The number of pulses

Figure 10 shows the relationship between the amplitude and the number of pulses for high flow conditions. This graph reveals that the number of pulses increases with increasing amplitude. The reason is that more particles exceed the threshold voltage, thus more particles are detected. Even though the number of pulses of the plate vibration sensor is much higher than the plate microphone one's due to the reason mentioned in 2.2.2, a significant difference is not found. The difference is that the plate microphone cannot detect $D_s < 2$ mm and 5 mm, respectively.

3.1.3 Acoustic energy and vibration energy

Figure 11 shows the acoustic energy (E_s) and the vibration energy (E_v) versus the BTR using low flow conditions. Here, the BTR is the weight used for each experiment divided by the observed time. The figure clearly depicts that the sediment of sizes $D_s = 2$ mm, 5 mm and 100 mm vary widely between zero and about 100 mV with a positive correlation of increasing E_v and E_s with increasing diameter. Even though the data of 5 mm and 10 mm gravels are distinguishable, 50 mm and 100 mm are not as they area in the same energy

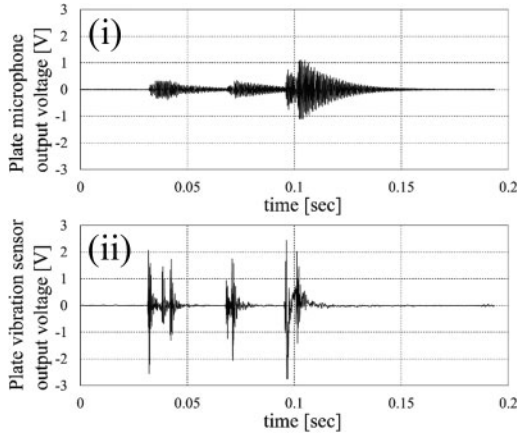


Figure 8. Waveform of case 10 ($V = 4.5$ m/s, $D_s = 100$ mm).

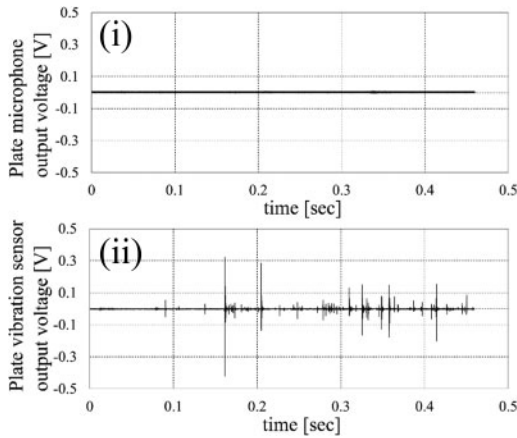


Figure 9. Waveform of case 6 ($V = 4.5$ m/s, $D_s = 2$ mm).

range. It can be concluded that the waves overlap when large sediment is transported. The results of acoustic energy also reveals that, by the plate microphone, only few of the $D_s = 2$ mm grains were detected. On the other hand, E_v of fine sediment has an almost constant value. This means that notwithstanding the detection of fine sediment are confirmed in the waveform data, were not reflected in the results of E_v . As the cause of this problem, it is possible that the threshold to measure E_v is too low for fine sediment to exceed. Therefore, this problem may be resolved by device adjusting.

3.2 Discussions

3.2.1 Detection rate

To know, how much sediment is detected by the devices compared to the total sediment amount, the detection rate R_d was defined as the number of detected pulsed divided by the number of particle used in one experiment (P_n). Figure 12 shows the relationship between R_d and the amplitude ($V = 2.5$ m/s). In general, R_d

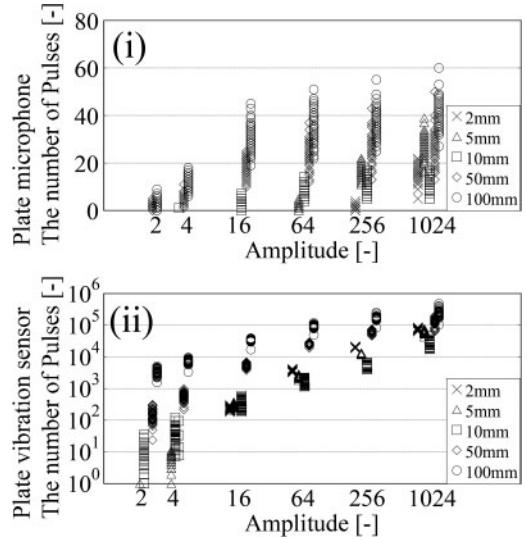


Figure 10. Results of the number of pulses ($V = 2.5$ m/s).

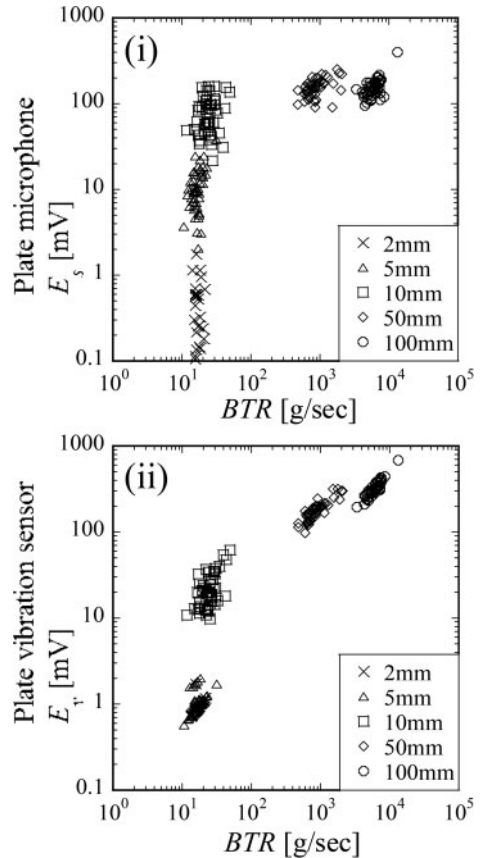


Figure 11. The acoustic energy (E_s) and the vibration energy (E_v) versus the bedload transport rate (BTR) ($V = 2.5$ m/s).

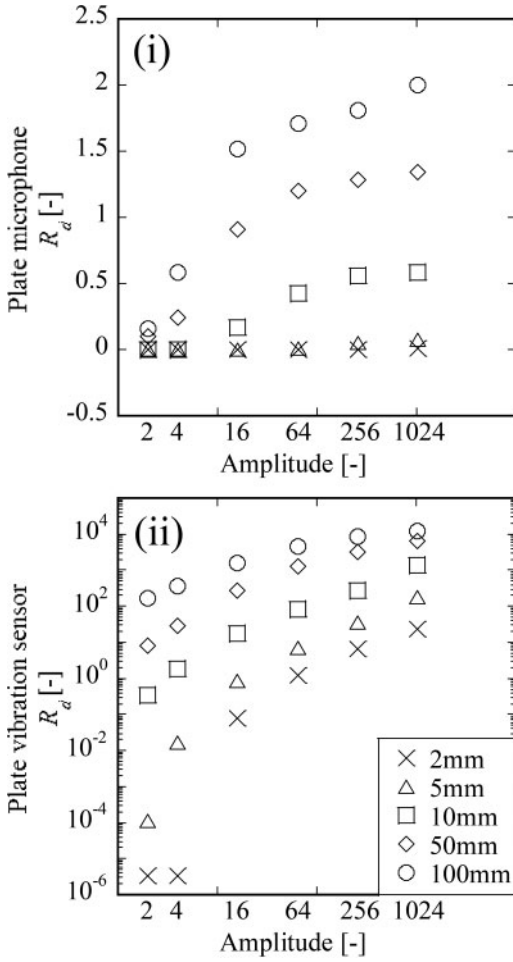


Figure 12. The relationship between the detection rate (R_d) and the amplitude. ($V = 2.5$ m/s).

increases with amplitude. The results of the plate microphone reveal that R_d of $D_s = 2$ mm and 5 mm are low, making it hard to estimate an accurate sediment transport rate. Especially, R_d of $D_s = 2$ mm with 2, 4, 16, and 64 times amplitude, $D_s = 5$ mm with 2, 4, and 16 times amplitude, and $D_s = 10$ mm with 2 times amplitude are zero. However, the detection rate for particles with $D_s > 10$ mm is good in general. On the other hand the results of the plate vibration sensor revealed that fine sediment less than 10 mm can be detected when the amplitude is high. Moreover, focusing on the amplitude larger than 4, R_d is increasing for all diameter of gravels.

3.2.2 Saturation rate

The detection rate can be calculated using the flow and sediment conditions. The number of sediment passing over the devices can be calculated by dividing the detected number of pulses by R_d . Therefore, two parameter governing R_d , namely the saturation rate R_s and hit probability $P(L_p)$ are introduced.

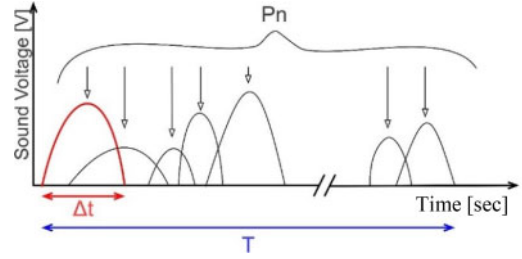


Figure 13. Parameters which compose saturation rate.

The saturation rate R_s is the number of particles transported over the plate at the same time representing a bulk density as:

$$R_s = \frac{\Delta t \times P_n}{T} \quad (1)$$

Here, Δt : impact time caused by one particle hit on the plate microphone [s], T : The time between first collision of first particle to the last of the last particle in one experiment. Figure 13 explains these parameters.

Figure 14 shows the relationship between R_d and R_s using amplitude larger than 4 for $D_s = 50$ mm at the low flow conditions. As R_s increases, R_d tends to decrease. When R_s rises, both the waveforms which interfere each other and the sediment transported without hitting on the plate microphone increase leading to a decreased value of R_d . This is confirmed for both devices but the results of the plate microphone with the low amplitudes does not show the negative correlation well. The reason of this can be expected that the pulses registered by the plate microphone tend to overlap because the each wave's length is generally longer than the plate vibration sensor's one as mentioned in 3.1.2.

3.2.3 Hit probability

It is obvious that the particle saltation length affects the relationship with R_d . Saltation length D_s for supercritical flows can be calculated as follows (Auel 2014):

$$\frac{L_p}{D_s} = 251\theta \quad (2)$$

Where, L_p : saltation length. θ : Shields parameter. θ is calculated by:

$$\theta = \frac{\tau_b}{\rho G_s g D_s} \quad (3)$$

where G_s : relative density, g : gravitational acceleration and shear stress τ_b is

$$\tau_b = \rho u_*^2 \quad (4)$$

where ρ : density of water and u_* : shear velocity:

$$u_* = \sqrt{ghi_b} \quad (5)$$

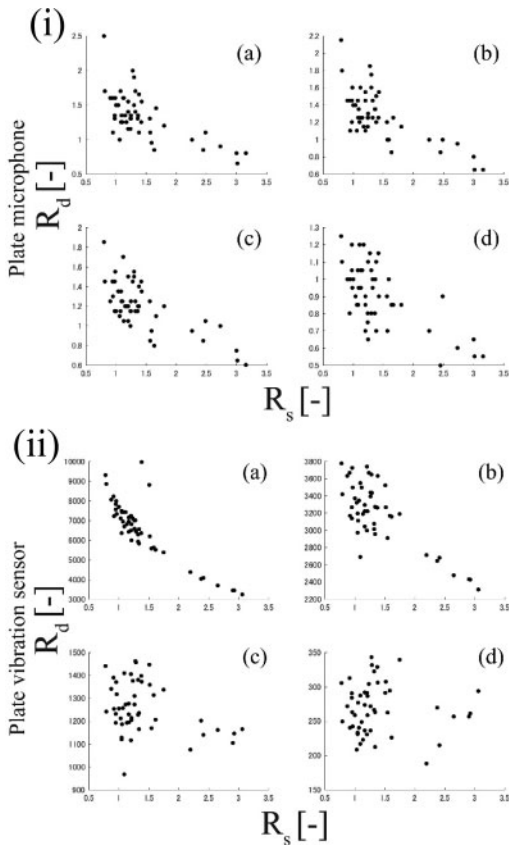


Figure 14. The relationship between the detection rate (R_d) and the saturation rate (R_s). ($D_s = 50$ mm, $V = 2.5$ m/s, amplitude of (a) = 1024, (b) = 256, (c) = 64 and (d) = 16).

With i_b = gradient of channel or energy line gradient. Since i_b of the flume in this experiment is 0° , i_b is represented by the energy gradient. Thus, probability based on saltation length $p(L_p)$ was calculated as follows:

$$P(L_p) = \frac{B}{L_p} \quad (6)$$

with B = plate length. Calculation results of Eq. (6) are shown in Figure 15, where R_d is given as a function of $P(L_p)$. The amplitude is 256 times and filled triangles mean $V = 4.5$ m/s, and filled circles mean $V = 2.5$ m/s.

Figure 15 reveals that $P(L_p)$ increases with decreasing fluid velocity for both devices as the arrows show. According to the result of the plate microphone, at high flow velocities, particles tend to jump very long and hence do not hit the plate often, whereas at low flow, particles tend to roll or only jump short distances and therefore show a higher detection rate R_d . However, particles $D_s = 50$ mm show satisfying $R_d = 1$ even for the high flow. That means that in average every particle hits the plate once although $P(L_p)$ is only about 20%. Consequently not only the saltation length but

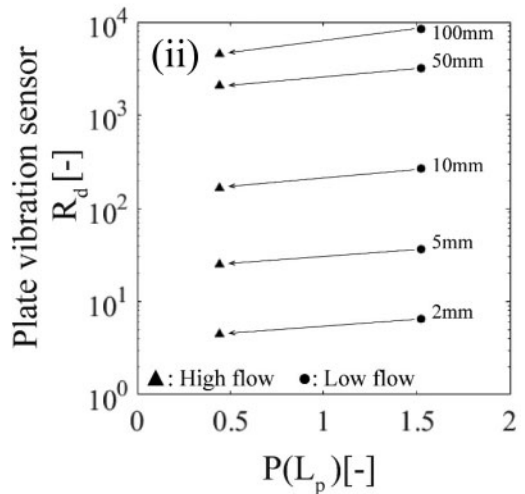
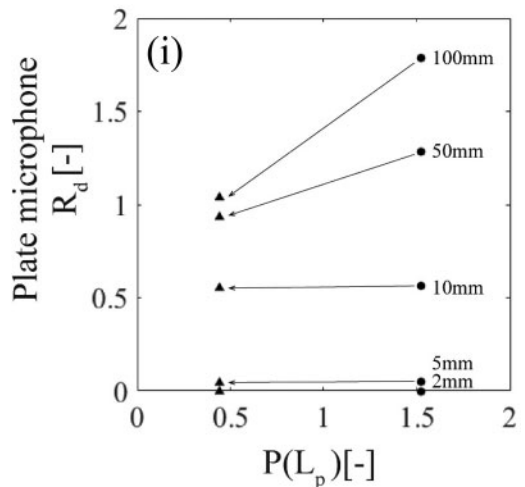


Figure 15. The relationship between the detection rate (R_d) and the hit probability ($P(L_p)$). (Amplitude = 256 times).

also the height has to be considered to calculate the hitting probability.

4 CONCLUSION

In this paper, two new systems to measure bedload transport rates, namely a plate microphone and a plate vibration sensor are introduced and compared experimentally. Both systems are developed based on existing systems, the Japanese hydrophone and Swiss geophone, in order to get over their weak points. As a consequence of the laboratory experiments, the following features of them are revealed. 1) The plate vibration sensor can detect fine sediment with the D_s smaller than 10 mm, which cannot be detected by the geophone. However, the plate microphone cannot detect fine sediment. 2) R_d is effective to calculate the bedload transport rate from the measured outputs.

3) Both devices outputs saturate when bedload transport rate is large. 4) In order to calculate the R_d from a given flow condition, R_s and the $P(Lp)$ are suggested and good correlation between the R_d and the parameters was found.

As a future study, more experiments to quantify the R_d by using the R_s and $P(Lp)$ are needed. At the same time, not only the minimum detectable grain size but also the maximum detectable grain size should be clarified. Moreover, these measuring methods are supposed to be installed at the outlet of Koshibu SBT in Nagano Prefecture in Japan. The SBT will start the operation from 2016 and in-situ experiments using Koshibu river sediments are planned before the commencement of the operation. Therefore, in the future, on site experiments and observations will be carried out in addition to the laboratory experiment to proceed a more pragmatic study.

ACKNOWLEDGEMENTS

The authors acknowledge the support of the VAW of ETH Zurich for excellent collaboration during the experimental calibration tests. Many thanks also go to the Ministry of Land, Infrastructure, Transport, and Tourism (MLIT) by sharing the information about the Koshibu SBT. This work was also supported by JSPS KAKENHI Grant Number 26257304 and by regional research project of river and sediment management technology development by MLIT. The second author acknowledges the support of the Japanese Society for the Promotion of Science.

REFERENCES

Auel, C., Kantoush, S.A. & Sumi, T. 2016. Positive effects of reservoir sedimentation management on reservoir life – examples from Japan. *84th Annual Meeting of ICOLD*, Johannesburg, South Africa.

Auel, C. 2014. Flow characteristics, particle motion and invert abrasion in sediment bypass tunnels. Doctoral dissertation No. 22008, ETH Zurich.

Auel, C. & Boes, R.M. 2011. Sediment bypass tunnel design – review and outlook. *Proc. ICOLD Symposium “Dams under changing challenges* (Schleiss, A.J. & Boes, R.M, eds.), 79th Annual Meeting, Lucerne. Taylor & Francis, London, UK: 403–412.

Baumer, A. & Radogna, R. 2015. Rehabilitation of the Palagnedra sediment bypass tunnel (2011–2013). *Proc. Int. Workshop on Sediment Bypass Tunnels*, VAW-Mitteilung 232 (Boes, R.M, ed.), ETH Zurich, Switzerland: 235–245.

Jacobs, F. & Hagmann, M. 2015. Sediment bypass tunnel Runcahez: Invert abrasion 1995–2014. *Proc. Int. Workshop on Sediment Bypass Tunnels*, VAW-Mitteilung 232 (Boes, R.M, ed.), ETH Zurich, Switzerland: 211–221.

Hagmann, M., Albayrak, I. & Boes, R.M. 2015. Field research: Invert material resistance and sediment transport measurements. *Proc. Int. Workshop on Sediment Bypass Tunnels*, VAW-Mitteilung 232 (Boes, R.M, ed.), ETH Zurich, Switzerland: 123–135.

Koshiba, T., Sumi, T., Takemon, Y. & Tsutsumi, D. 2016. Flume Experiment on Bedload Measurement with a Plate Microphone. *Annuals of Disaster Prevention Research Institute, Kyoto University*, No. 58B: 458–469.

Mizuyama, T., Matsuoka, M. & Nonaka, M. 2008. Bedload measurement by acoustic energy with Hydrophone for high sediment transport rate. *Journal of the Japan Society of Erosion Control Engineering*, 61(1): 35–38 (in Japanese).

Mizuyama, T., Oda, A., Laronne, J.B., Nonaka, M. & Matsuoka, M. 2010. Laboratory tests of a Japanese pipe geophone for continuous acoustic monitoring of coarse bedload. *US Geological Survey Scientific Investigations Report*, 5091: 319–335.

Nakajima, H., Otsubo, Y. & Omoto, Y. 2015. Abrasion and corrective measures of a sediment bypass system at Asahi Dam. *Proc. Int. Workshop on Sediment Bypass Tunnels*, VAW-Mitteilung 232 (Boes, R.M, ed.), ETH Zurich, Switzerland: 21–32.

Rickenmann, D., Turowski, J.M., Fritschi, B., Klaiber, A. & Ludwig, A. 2012. Bedload transport measurements at the Erlenbach stream with geophones and automated basket samplers. *Earth Surface Processes and Landforms*, 37(9): 1000–1011.

Schwalt, M. & Hager, W.H. 1992. Die Strahlbox (The jet-box). *Schweizer Ingenieur und Architekt* 110(27/28): 547–549 (in German).

Sumi, T., Okano, M. & Takata, Y. 2004. Reservoir sedimentation management with bypass tunnels in Japan. *Proc. 9th International Symposium on River Sedimentation*, Yichang, China: 1036–1043.

Suzuki, T., Mizuno, H., Osanai, N., Hirasawa, R. & Hasegawa, Y. 2010. Basic study on sediment rate measurement with a hydrophone on the basis of sound pressure data. *Journal of the Japan Society of Erosion Control Engineering*, 62(5): 18–26.

Tsutsumi, D., Hirasawa, R., Mizuyama, T., Shida, M. & Fujita, M. 2010. Bed Load Observation in a Mountainous Watershed by Hydrophone Equipments. *Annuals of Disaster Prevention Research Institute, Kyoto University*. No. 53 B: 537–543 (in Japanese).